SH wave modelling by a staggered-grid method

Zaiming Jiang, John C. Bancroft, and Laurence R. Lines

ABSTRACT

Theory and technology of a staggered-grid finite-difference method on SH wave modelling is reviewed. The ingredients of the modelling method, including finite-difference scheme, seismic sources, free-surface boundary conditions, and computational boundary conditions, are discussed.

In addition, modelling results are interpreted to investigate the advantages and disadvantages of the modelling method, and to demonstrate some processing and interpolation related wave phenomena and seismological principles, such as guided surface waves, the problem of seismic resolution, geometrical spreading, and seismic multiple reflections.

INTRODUCTION

Seismic modelling plays an important role in data acquisition, processing, and interpretation. Uses of seismic modelling include design of seismic experiments, prediction of seismic results, enchancing interpretation, inversion, testing processing algorithms, and examining effects of noise (Lines and Newrick, 2005).

Among various modelling methods, such as normal-incidence reflectivity methods, Zoeppritz's equation methods, ray tracing, and physical modelling, finite-difference methods can offer more general and complete seismic modelling results.

It is important to study shear-horizontal (SH) wave, in addition to the more popular P-SV case. "The fact that surface SH waves are observed in nature has been used to infer that the Earth's crust is layered." (Krebes, 2006). Also, recent development in oil industry, such as oil sands exploration and monitoring, involves more and more multi-component surveys.

Finite-difference modelling methods can be classified in two broad categories: staggered-grid and non-staggered grid. The classical paper about non-staggered grid methods is by Kelly et al. (1976), while two classical papers about staggered-grid methods are by Virieux (1984, 1986).

This report begins with the review of SH wave modelling based on Virieux's staggered-grid scheme (Virieux, 1984). In addition to the finite-difference method itself, the other technologies, such as seismic source modelling, free-surface boundary conditions, and computational boundary conditions are also discussed, since they are integral parts of this method.

The discussion is followed by interpretations of modelling results. Guided surface SH waves, seismic resolution, geometrical spreading, and seismic wave multiple reflections are demonstrated.

THEORY AND IMPLEMENTATION

A staggered-grid scheme for SH wave modelling

Combining equation of motion and stress-strain relation for isotropic elastic media, we obtain the elastodynamic equations as followings.

$$\begin{cases} \rho\frac{\partial^2 u_i}{\partial^2 t} = \sum_{j=1}^{3}\frac{\partial \sigma_{ij}}{\partial x_j}, & i=1,2,3, \\ \sigma_{ij} = \lambda\mathcal{D}\delta_{ij} + 2\mu e_{ij}, & i,j=1,2,3, \end{cases} \tag{1}$$

where ρ is density, u_i is a displacement component, σ_{ij} is a stress tensor, $\mathcal{D} = \sum_k e_{kk}$ is the dilatation, λ and μ are Lam*é* constants, δ_{ij} is the Kronecker delta, and e_{ij} is a strain tensor. In the equation system (1), the first is the equation of motion, and the second one is the stress-strain relation.

Substitution of the the stress-strain relation into the equation of motion leads to the homogeneous or heterogeneous formations of 2D wave equation system used by Kelly et al(1976), or the acoustic wave equations for compressional waves and transverse waves with different dimensions.

Alternatively, the equation system (1) can be transformed into different velocity-stress systems of waves for 1D P-wave case, 1D S-wave case, 2D P-SV wave case, 2D SH wave case, and 3D case. (Note that in the term 'velocity-stress', 'velocity' refers to the particle velocity.) 2D P-SV wave modelling has been sucessfully used in our reverse-time migration algorithms (Jiang et al., 2009). This report is about 2D SH case.

The 2D SH wave velocity-stress system is obtained as

$$\begin{cases} \rho\frac{\partial v_2}{\partial t} = \frac{\partial \sigma_{12}}{\partial x_1} + \frac{\partial \sigma_{23}}{\partial x_3}, \\ \frac{\partial \sigma_{12}}{\partial t} = \mu\frac{\partial v_2}{\partial x_1}, \\ \frac{\partial \sigma_{23}}{\partial t} = \mu\frac{\partial v_2}{\partial x_3}. \end{cases} \tag{2}$$

where v_2 is the shear horizontal particle velocity.

If a same grid step h is used for both x_1 and x_3 axes and Δt is used for the time step, a discrete form of equation (2) is

$$\begin{cases} {v_2}_{i,k}^{n+1/2} = {v_2}_{i,k}^{n-1/2} + \frac{\Delta t}{h\rho_{i,k}}\left({\sigma_{12}}_{i+1/2,k}^{n} - {\sigma_{12}}_{i-1/2,k}^{n} + {\sigma_{23}}_{i,k+1/2}^{n} - {\sigma_{23}}_{i,k-1/2}^{n}\right), \\ {\sigma_{12}}_{i+1/2,k}^{n+1} = {\sigma_{12}}_{i+1/2,k}^{n} + \frac{\mu_{i+1/2,k}\Delta t}{h}\left({v_2}_{i+1,k}^{n+1/2} - {v_2}_{i,k}^{n+1/2}\right), \\ {\sigma_{23}}_{i,k+1/2}^{n+1} = {\sigma_{23}}_{i,k+1/2}^{n} + \frac{\mu_{i,k+1/2}\Delta t}{h}\left({v_2}_{i,k+1}^{n+1/2} - {v_2}_{i,k}^{n+1/2}\right), \end{cases} \tag{3}$$

where i is the index for x_1 discretization, k is the index for x_3 discretization, and n is the index for time discretization. A schematic diagram of the staggered-grid is shown in Figure 1.

Seismic source scheme

Ricker wavelets are introduced into the staggered-grid onto a particle velocity node as shown in Figure 2.

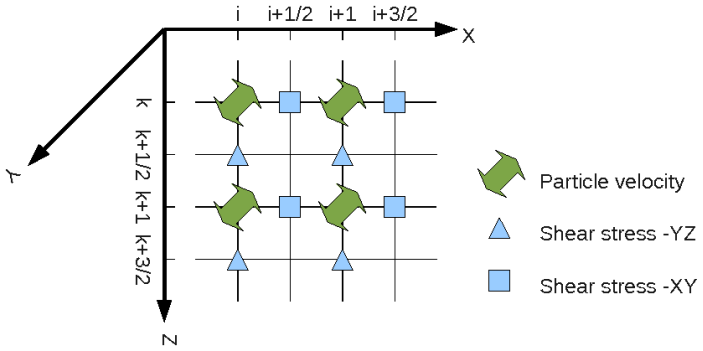

FIG. 1: Staggered-grid for SH wave modelling

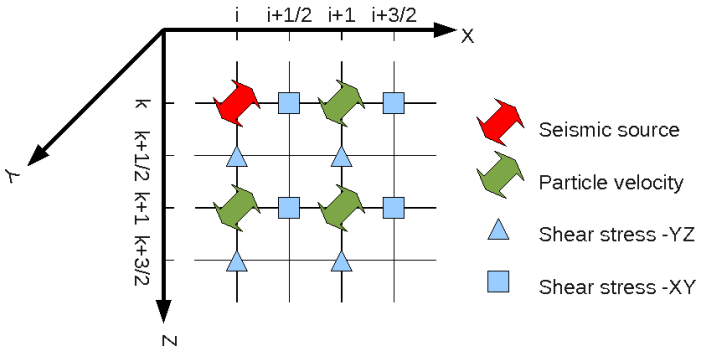

FIG. 2: Introducing seismic source into a staggered grid

Seismic resolution is related to seismic source frequencies. Ricker wavelets with two different peak frequencies are shown in Figure 3. The wavelets are shown in time. One can expect that they have different spatial wavelengths when they propagate in rocks.

Free surface boundary condition

The earth surface is stress-free. That is, the normal stresses must be zero at the surface. In 2D SH wave case, this boundary condition can be denoted as

$$\sigma_{23} = 0. \tag{4}$$

The discretization form of equation (4) in our specified grid is

$$\sigma_{23}\Big|_{-1/2} = -\sigma_{23}\Big|_{1/2}, \tag{5}$$

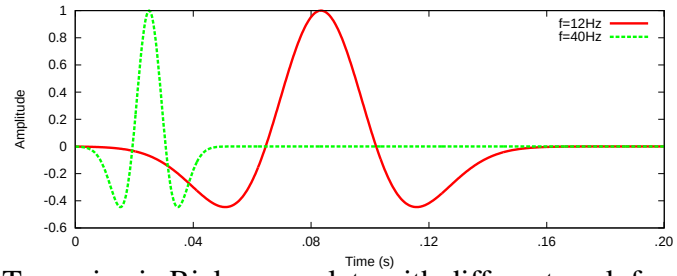

FIG. 3: Two seismic Ricker wavelets with different peak frequencies

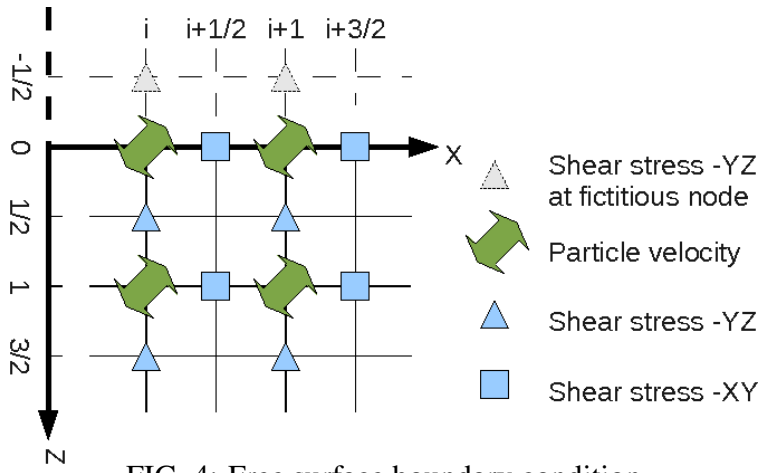

FIG. 4: Free surface boundary condition

where subscript $-1/2$ denotes a fictious stress node about the surface. Since this boundary condition is true at any time at any place on the surface, the both indices for time and offset are ignored. The schematic diagram is shown in Figure 4.

Using the boundary condition, one can calculate fictious stresses above the surface, which in turn, can be used to calculate particle velocities on the free surface at the next half time step. Note that the only surface boundary condition is about stress, not about displacement (or velocity) of the particles.

Computational boundary conditions

To reduce the artificial reflections that are introduced by the edge of the computational grid, a method of combining absorbing boundary conditions (Clayton and Engquist, 1977) and nonreflecting boundary condition (Cerjan et al., 1985) is applied to the sides and bottom of subsurface models. For details about the combined boundary conditions, please refer to the abstract (Jiang et al., 2010).

MODELLING RESULTS

To check the correctness and effectiveness of the implementations of the finite-difference method, the seismic source scheme, the free surface boundary condition, and the computational boundary conditions, a few subsurface models are created, and the modelling results are shown. At the same time, by analyzing these results one might gain some perceptual knowledge about guided surface SH waves, seismic resolution problem, geometrical spreading, and seismic wave multiples.

A homogeneous subsurface with a buried seismic source

The first subsurface model is a $750m$x$750m$ homogeneous medium, with S-wave velocity of $2020.73m/s$ and density of $2380.90kg/m^3$. The grid spactial step is $1.25m$, and the time step is $0.00025s$.

By burying a seismic source at the centre of the model and firing it, a shear wave is

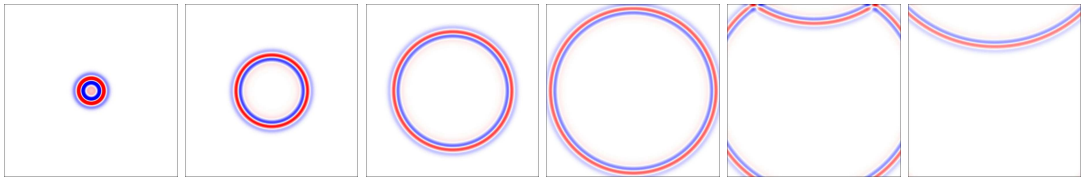

(a) t=0.05s (b) t=0.10s (c) t=0.15s (d) t=0.20s (e) t=0.25s (f) t=0.30s

FIG. 5: SH wave in a homogeneous media, with a buried seismic source

generated and it propagates outwards. Figure 5 shows the wave propagation. When the shear wave hits the bottom and both left and right sides of the subsurface model, it just disappears. When the wave reaches the surface from the bottom of the surface, reflections are generated, and it could be observed that the amplitude of the reflection is approximately the same as that of the incident.

Obviously the computational boundary conditions applied on the bottom and both the left and the right sides of the subsurface work very well, since there is no noticeable reflections generated from these boundaries.

Are the surface reflections correct? Let us find the answer by checking into the reflection coefficients upon the surface. Let $u^{(I)}$ and $u^{(R)}$ denote, respectively, the incident and reflected wave displacement at an interface of two media for a normally incidence case, ρ_1 and ρ_2 are, respectively, the densities of the first and the second media, and β_1 and β_2 are, respectively, the wave velocities of the first and the second media. From the stress-strain relation one can derive that

$$u^{(R)} = -Ru^{(I)}, \tag{6}$$

where R is the particle displacement reflection coefficient at the interface of the two media:

$$R = \frac{\rho_2\beta_2 - \rho_1\beta_1}{\rho_2\beta_2 + \rho_1\beta_1}. \tag{7}$$

For an upgoing wave normally striking a ground surface from the bottom of the surface, the second medium is air, where $\rho_2 \approx 0$. Therefore, the reflection coefficient is $R \approx -1$ and $u^{(R)} \approx u^{(I)}$. In physical terms, this means that the wave propagation direction has flipped, but there is no amplitude reduction or polarity reversal in the displacement upon reflection from a free surface (Krebes, 2006). This is what we have observed from the modelling results. Thus, one can conclude that the free surface boundary condition in the implementation works correctly.

A homogeneous subsurface with a surface seismic source

Putting a seismic source at the surface centre of the same subsurface model as the last subsection, SH wave is generated and it propagates downwards. Figure 6 shows the wave propagation.

The distances that wave peaks travelled at different modelling times are shown in table 1. It could be calulated that the modelled waves travel at the velocity of $2020.00m/s$, which

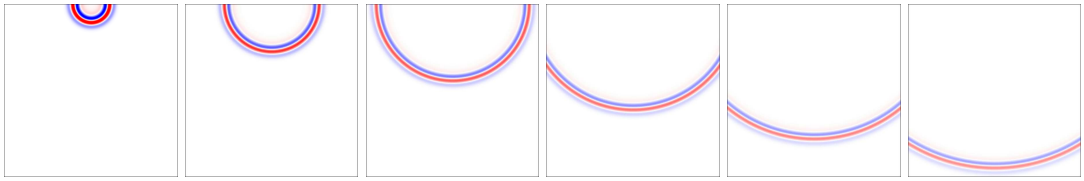

(a) t=0.0625s (b) t=0.1250s (c) t=0.1875s (d) t=0.2500s (e) t=0.3125s (f) t=0.3750s

FIG. 6: SH wave in a homogeneous media, with a surface seismic source

is very close to the specified value in the subsurface model. That is, the finite-difference method implicitly implements the propagation velocity of a SH wave.

Table 1: Travel time, disctances, and amplitudes

Figure	Time (s)	Distance (m)	Amplitude	$Amplitude \times \sqrt{distance}$
6a	0.0625	80.00	0.02416	0.216
6b	0.1250	206.25	0.01495	0.215
6c	0.1875	332.50	0.01169	0.213
6d	0.2500	458.75	0.00986	0.211
6e	0.3125	585.00	0.00863	0.209
6f	0.3750	711.25	0.00773	0.206

In addition, from the calculation results of $Amplitude \times \sqrt{distance}$ shown in table 1, one can find that the amplitude scales as $\frac{1}{\sqrt{distance}}$. This is different from the spherical wave propagation in the 3D real world , where amplitude scales as $\frac{1}{distance}$. Books, such as Shearer (1999), have explained in detail about the amplitude-distance relation for spherical waves. One can apply the same principles to explain the amplidute-distance relation for cirlular waves in two dimensional modelling.

Although there are amplitude differences between the 3D real world and 2D modelling, most of the time, this does not cause problems when we utilize 2D algorithms to process seismic data from the 3D world. However, for amplitude sensitive technologies, such as AVO, we need to have the concept of amplitude differences in mind.

We can make another interesting observation on this modelling experiment: there is no surface wave generated in this experiment, which is different from modelling experiments of P-SV case. However, this is consistent to the theoritical predictions: "surface SH waves cannot exist on the surface of a homogeneous half-space" (Krebes, 2006). Analysis also tells us, though, surface SH waves can exist on the surface of an inhomogeneous half-space. The next subsection of this report is about an experiment with an inhomogeneous medium, and we can check into surface SH waves.

A surface layer above a high velocity half-space

The surface layer model contains two layers: the surface layer is a low wave velocity medium, and below the surface layer is a high speed half-space. For detailed geometry

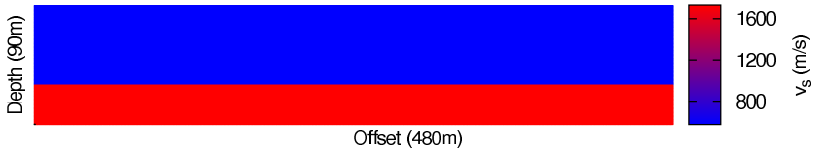

FIG. 7: A surface layer above a high speed half-space

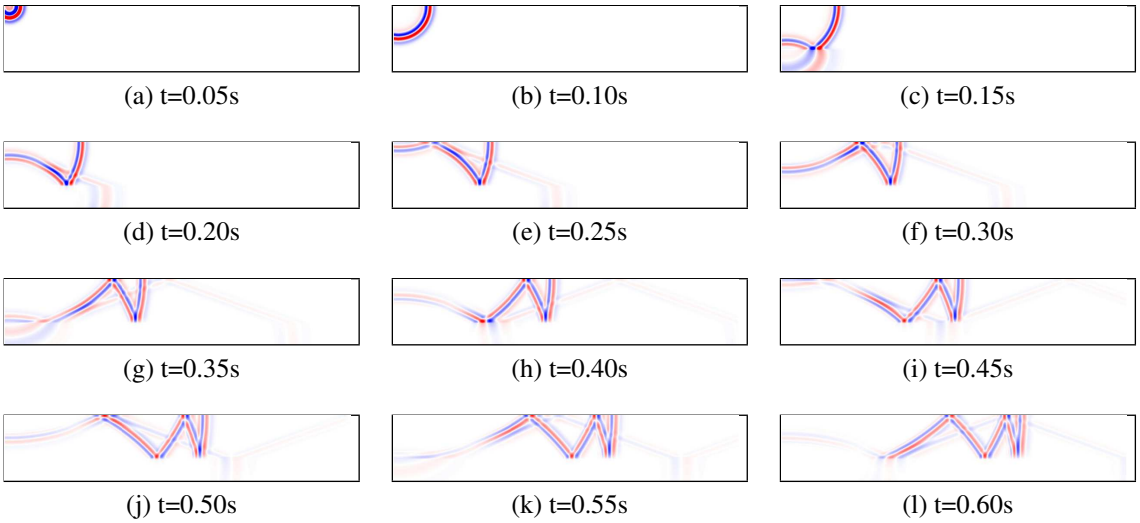

FIG. 8: SH wave in a surface laryer model

and rock properties of the model, please refer to Table 2 and Figure 7. The numerical grid spatial step is $0.6m$, the time step is $0.0001s$. The total modelling time is $0.6001s$

Table 2: A surface layer above a high velocity half-space

Layer	S-Wave volocity (m/s)	Density (kg/m^3)	Thickness(m)
Surface layer	577.35	1740.70	60
High velocity half-space	1732.05	2290.89	30

In the modelling experiment, a seismic source is placed close to the top-left corner on the surface. Snapshots from the modelling are show in Figure 8. From the snapshots, one can identify direct arrivals, primary reflected waves, transmitted waves, header waves, and multiple reflections. Significantly, most of the wave energe is trapped inside the surface layer and the surface layer acts as a wave guide. That is why the waves are called guided waves.

A thin layer model

"How thin is a thin layer?" This is a question posed in a paper (Widess, 1973) and then referenced in a book (Lines and Newrick, 2005). This is a problem of seismic resolution. By analysising our modelling results, we can gain some perceptual knowledge about this problem.

In the subsurface model shown in Figure 9, a thin layer is presented in surrounding

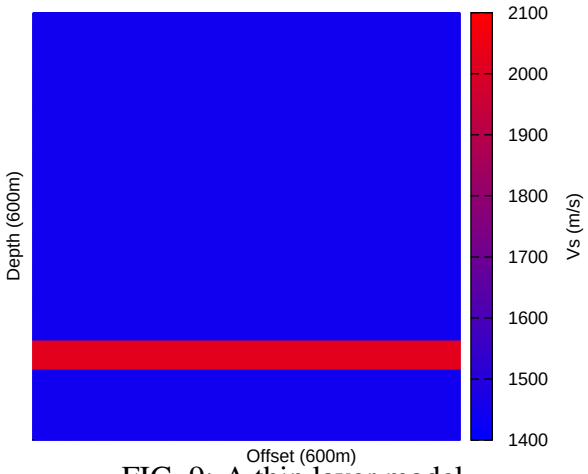

FIG. 9: A thin layer model

rocks. The thickness of the thin layer is $41m$. The overburden rock has a thickness of $460m$. The S-wave velocities of the thin layer and the sursounding rock are, respectively, $1443.38m/s$ and $2020.73m/s$. The densities are $2188.82kg/m^3$ and $2380.90kg/m^3$. The grid spatial step is $1m$, and the time step is $0.0002s$.

Two seismic experiments are done with the seismic sources being put on the surface centre. The only diffference is the peak frequencies of the seismic sources: one is of $12Hz$, while the other is of $40Hz$. Note that since the relation between wavelength, velocity and frequency $\lambda = \frac{v}{f}$, a $12Hz$ signal in a medium of S-wave velocity being $2020.73m/s$ has a wave length of approximately $163m$, which is as four times long as the thickness of the thin layer. While a signal of $40Hz$ has a wave length of approximately $50.5m$, which is close to $\frac{5}{4}$ times of the thickness of the thin layer.

Figure 10 shows surface records from the two seismic experiments. Direct arrivals appears as linear events on the uppper parts of the records, and reflection events appears as hypobolas on the lower parts. On the surface record of low frequency seismic source (Figure 10a), one can only identify one reflection event. However, on the record of high requency source (Figure 10b), the two relection events are completely separated into two hypobolas.

How thin is a thin layer? The answer is that it depends on the wave length of a seismic signal, which in turn, depends on the wave velocities in media and seismic frequencies. The higher the peak frequency of the seismic source and the lower the wave velocity in media, the better one can distinguish thin media layers. For a certain medium, we cannot change the wave velocity, but we can utilize seismic sources of higher frequencies to gain higher resolution survey results.

CONCLUSIONS

Various aspects, such as staggered-grid scheme, free-surface boundary condition, computational boundary conditions, and seismic sources, of a SH wave modelling method are discussed. Modelling results show that the implementation is accurate. Also we tried to connect the modelling results to seismic wave phenomena and seismological principles,

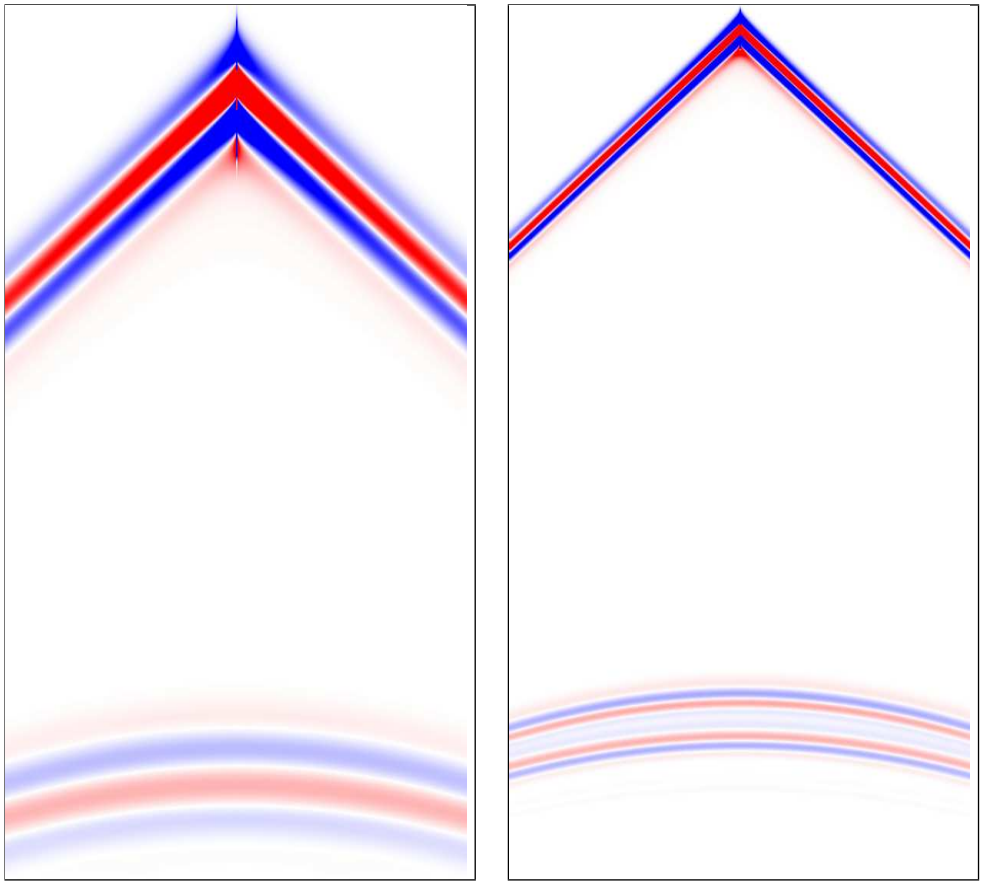

(a) f=12Hz (b) f=40Hz

FIG. 10: Surface records generated from different source peak frequencies using a thin layer model

with the expectation of gaining some perceptual knowledge.

ACKNOWLEDGEMENTS

We thank the sponsors of CREWES for their continued support.

REFERENCES

Cerjan, C., Kosloff, D., Kosloff, R., and Reshef, M., 1985, A nonreflecting boundary-condition for discrete acoustic and elastic wave-equations: Geophysics, **50**, No. 4, 705–708.

Clayton, R., and Engquist, B., 1977, Absorbing boundary-conditions for acoustic and elastic wave-equations: Bulletin of the Seismological Society of America, **67**, No. 6, 1529–1540.

Jiang, Z., Bancroft, J. C., and Lines, L. R., 2010, Combining absorbing and nonreflecting boundary conditions for elastic wave modeling: SEG Eightieth Annual Meeting Expanded Abstract, 2935–2939.

Jiang, Z., Bancroft, J. C., Lines, L. R., and Hall, K. W., 2009, Elastic prestack reverse-time migration using a staggered-grid finite-difference method: CREWES Research Report, **21**.

Kelly, K. R., Ward, R. W., Treitel, S., and Alford, R. M., 1976, Synthetic seismograms - finite-difference approach: Geophysics, **41**, No. 1, 2–27.

Krebes, E. S., 2006, Seismic theory and methods: University of Calgary.

Lines, L. R., and Newrick, R. T., 2005, Fundamentals of Geophysical Interpretation: Society of exploration geophysicists publication, Tulsa, Oklahoma.

Shearer, P. M., 1999, Introduction to seismology: Cambridge University Press.

Virieux, J., 1984, Sh-wave propagation in heterogeneous media - velocity-stress finite-difference method: Geophysics, **49**, No. 11, 1933–1942.

Virieux, J., 1986, P-sv wave propagation in heterogeneous media: Velocity-stress finite-difference method: Geophysics, **51**, No. 4, 889–901.

Widess, M., 1973, How thin is a thin bed: Geophysics, **38**, No. 6, 1176–1180.